# EXTENSION OF DISCRETE-TIME FLUTTER PREDICTION METHOD TO A HIGHER-MODE SYSTEM

Hiroshi Torii[+1]
Meijo University, Nagoya, Japan

Conventionally flutter boundaries have been predicted based on the modal damping. However, the accurate estimation of damping is difficult and, in some cases, the damping coefficient is not necessarily an appropriate measure for the flutter prediction. To overcome the defect of the damping method, authors proposed an alternative parameter, the flutter margin for discrete-time systems (FMDS), which is approximately equivalent to Zimmermann's flutter margin, and has suitable properties as the flutter prediction parameter. Since it was applicable only to the binary flutter, we have attempted to extend the FMDS so as to be applicable to a higher-mode system. In this paper we give an overview of FMDS and attempt its extension to a higher-mode system.

**Keyword**: flutter prediction, flight testing, ARMA model, flutter margin

## 1. INTRODUCTION

Since flutter is the self excited vibration which causes a fatal damage to an airfoil, we have to pay utmost attention to the occurrence of flutter in the airplane design and development. At the final stage of airplane development, therefore, wind tunnel and flight tests are conducted to check that flutter does not occur in the flight envelop, and to evaluate the flutter boundary speed. Since the flutter tests are generally carried out in the safety range far below the critical point to avoid structural damage during the tests, the flutter boundary is predicted from the behavior of some stability criteria plotted against flight speed or dynamic pressure as shown in Fig.1. The stability margin has been conventionally evaluated by damping of aeroelastic modes. For a reliable prediction of flutter, it is quite significant to measure the modal damping as accurate as possible from flight test data. However an accurate evaluation of damping of a wing in an airstream is not necessarily an easy task, so that lots of works on the flutter prediction have been directed to improve the accuracy or

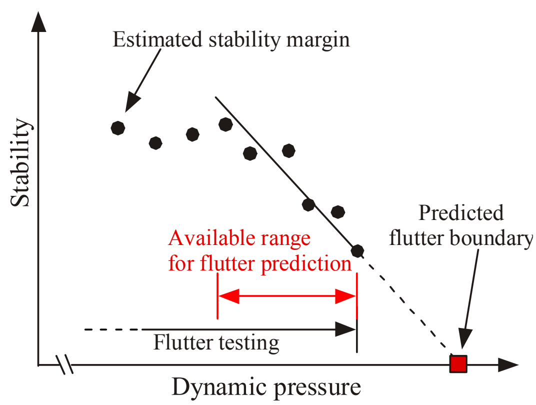


Figure 1: Flutter prediction

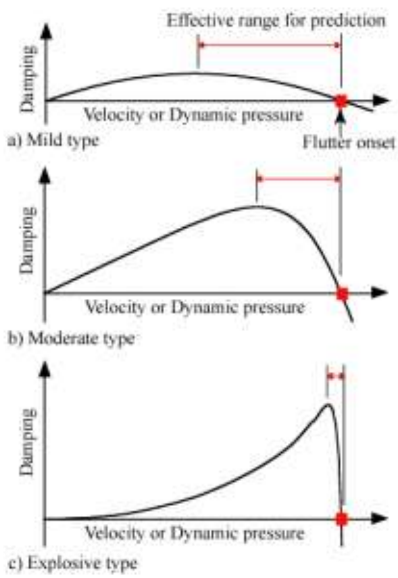


Figure 2: Behavior of damping

[+1]htorii@meijo-u.ac.jp

efficiency of damping estimation. It is pointed out, however, that damping is not always an appropriate index to predict the flutter boundary[1)]. Figure 2 depicts the behavior of damping against the dynamic pressure for three types of flutter. For the explosive type of flutter, it shows that damping gives no sign of instability up to the neighborhood of the critical speed.

As an alternative approach, Zimmerman and Weissenburger[1)] attempted to propose a more suitable parameter for the flutter prediction than damping, and introduced "Flutter Margin". It is derived from Routh's stability test, which is a method to check the stability of system based on the characteristic equation. The parameter decreases almost monotonically toward zero as the dynamic pressure increases. This is a very favorable property for the flutter prediction. However, it is applicable only to binary-flutter. The extension to a three-mode system was attempted by Price and Lee[2)].

Since the Flutter Margin is defined based on the continuous-time system, it is not convenient for digital processing. In the discrete-time domain, Matsuzaki and Ando[3)] proposed to use Jury's stability parameters as the indicator of stability margin, which is stability criteria for the discrete-time system and are calculated from the discrete-time characteristic equation. Jury's stability parameter starts to decrease at lower speed range than damping, but it is sensitive to the noise and filter setting. Then authors [4)] modified Jury's parameters and introduced the new indicator called "Flutter Margin for the Discrete-time System (FMDS) ". We showed that it was approximately equivalent to Zimmerman's Flutter Margin, so that it decreases almost monotonically as the dynamic pressure increases for the simple two-dimensional wing model. Though the FMDS has superior properties as the flutter prediction parameter, it is applicable to the data which include only two coupling modes similarly to Flutter Margin. This limitation should be relaxed to make FMDS method practicable to the flutter tests. Bae et al.[5)] attempted the extension of the FMDS to the multimode system. As mentioned by McNamara and Friedmann[6)], however, a mathematical foundation or a theoretical consideration of the parameter introduced is not given in Ref.5, and furthermore it is not consistent with the FMDS for the two-mode system. Therefore the extension of the FMDS is still an open problem.

The purpose of this work is to extend the FMDS to the three-mode system. A new flutter prediction parameter is proposed based on Jury's stability determinant method. The properties of the parameter are investigated using wing models with three- and four-modes. Then to check the feasibility for an actual data we show the application results to the wind tunnel flutter test data which are measured under the stationary and non-stationary conditions.

## 2. REVIEW OF FLUTTER PREDICTION METHODS

In this section we will review Zimmermann's Flutter Margin[1)], Jury's stability parameter method[3)], and FMDS[4)].

### (1) Flutter Margin

From the modal damping and frequency, we can obtain the characteristic roots of the j-th mode.

$$s_j = \alpha_j + i\beta_j, \quad s_j^* = \alpha_j - i\beta_j$$

The equation corresponding to the roots, $s_j$ and $s_j^*$, is expressed as follows.

$$(s - s_1)(s - s_1^*)(s - s_2)(s - s_2^*) = 0$$

The expansion of it gives the following characteristic equation.

$$s^4 + P_3 s^3 + P_2 s^2 + P_1 s + P_0 = 0 \tag{1}$$

Combining Routh's stability parameters for Eq.1, Zimmermann defined the flutter margin:

$$F = -\left(\frac{P_1}{P_3}\right)^2 + P_2\left(\frac{P_1}{P_3}\right) - P_0 \qquad (2)$$

The value of $F$ indicates the stability margin, that is, $F$ is positive in the subcritical speed range and becomes zero at the flutter boundary. Using the relation between roots and coefficients of equation, Eq.2 is also expressed as follows.

$$F = \left\{\left(\frac{\beta_2^2-\beta_1^2}{2}\right)+\left(\frac{\alpha_2^2-\alpha_1^2}{2}\right)\right\}^2 + 4\alpha_1\alpha_2\left\{\left(\frac{\beta_2^2+\beta_1^2}{2}\right)+2\left(\frac{\alpha_2^2+\alpha_1^2}{2}\right)^2\right\}$$
$$-\left\{\left(\frac{\alpha_2-\alpha_1}{\alpha_2+\alpha_1}\right)\left(\frac{\beta_2^2-\beta_1^2}{2}\right)+2\left(\frac{\alpha_2^2+\alpha_1^2}{2}\right)^2\right\}^2$$

This is a convenient expression to evaluate the value of $F$ from the aeroelastic characteristics estimated at the experiments. Moreover, from the analysis using a two-dimensional wing model with a quasi-steady aerodynamics, the Flutter Margin is shown to be a quadratic function of the dynamic pressure $q$.

$$F = C_2\left(C_{L_\alpha}q\right)^2 + C_1\left(C_{L_\alpha}q\right) + C_0 \qquad (3)$$

**(2) Jury's stability parameter**

Nowadays we generally acquire and treat data at a digital form. Since the Flutter Margin, however, is defined in the continuous-time domain, it is not adequate to cope with such a digital system. In Ref.3 Matsuzaki proposed to use Jury's stability criteria to measure the stability margin.

Using the time-series analysis method, sampled data $\{y_1, y_2, y_3, ...\}$ can be identified by the following Autoregressive Moving Average (ARMA($n$, $m$) ) model.

$$y_t + \alpha_1 y_{t-1} + \alpha_2 y_{t-2} + \cdots + \alpha_n y_{t-n} = e_t + \beta_1 e_{t-1} + \beta_2 e_{t-2} + \cdots + \beta_{t-m} e_{t-m}$$

where $y_t$ is the data observed at time $t$, $e_t$ a white noise. The order $n$ of AR part (the left hand side) is twice the number of vibration modes $M$, that is, $n$=2$M$, and the order $m$ of MA part (the right hand side) is less than $n$. Generally the optimal order $n$ and $m$ are decided by the Akaike Information Criteria (AIC). The AR part corresponds to the following characteristic polynomial of the discrete-time system.

$$G(z) = z^{2M} + \alpha_1 z^{2M-1} + \cdots + \alpha_{2M-1}z + \alpha_{2M} = \sum_{i=1}^{M}(z-z_i)(z-z_i^*)$$

where $z_i$ is the characteristic root of the i-th mode, and the root with a superscript * is the complex conjugate.

According to Jury's stability test (determinant method), the system is stable if and only if all the following conditions are satisfied.

$$G(1) = 1 + \alpha_1 + \cdots + \alpha_{2M-1} + \alpha_{2M} > 0$$
$$G(-1) = 1 - \alpha_1 + \cdots - \alpha_{2M-1} + \alpha_{2M} > 0$$
$$F_k^+ = \det\left(X_k + Y_k\right) > 0, \quad (k = 1, 3, \cdots 2M-1)$$
$$F_k^- = \det\left(X_k - Y_k\right) > 0, \quad (k = 1, 3, \cdots 2M-1)$$

where matrices $X_k$ and $Y_k$ are

$$X_k = \begin{pmatrix} 1 & \alpha_1 & \cdots & \alpha_{k-1} \\ 0 & 1 & \ddots & \vdots \\ \vdots & \ddots & \ddots & \alpha_1 \\ 0 & \cdots & 0 & 1 \end{pmatrix}, \quad Y_k = \begin{pmatrix} \alpha_{n-k,1} & \cdots & \alpha_{n-1} & \alpha_n \\ \vdots & \iddots & \alpha_n & 0 \\ \alpha_{n-1} & \iddots & \iddots & \vdots \\ \alpha_n & 0 & \cdots & 0 \end{pmatrix}$$

In the flutter test, the system is stable at the subcritical speed range, so that all the above conditions are satisfied. At the flutter boundary the system becomes unstable, and one of the values reaches zero. Among them, parameter $F^{-}_{2M-1}$ is expressed as follows[7].

$$F^{-}_{2M-1} = \prod_{i<j}^{2M} (z - z_i z_j) = \prod_{i<j}^{M} (1 - |z_i|^2) \times f(z_1, \cdots, z_{2M}) \tag{4}$$

where $z_{M+i} = z_i^*$ for $i$=1, 2, ... $M$, and $f(z_1,...,z_{2M})$ includes the remaining terms, which does not become zero at the flutter boundary. Because of the first factor in the right hand side of Eq.4, this parameter becomes zero when one of $z_i$ reaches a unit circle, that is, the occurrence of flutter. Therefore we can use $F^{-}_{2M-1}$ for the flutter prediction, and this is Jury's stability parameter proposed in Ref.3

**(3) Flutter Margin for the Discrete-time System (FMDS)**

After preprocessing through the band-pass filter so as to include only the coupling mode which causes flutter, sampled data is identified by the ARMA(4, *m*) model

$$y_t + \alpha_1 y_{t-1} + \alpha_2 y_{t-2} + \alpha_3 y_{t-3} + \alpha_4 y_{t-4} = e_t + \beta_1 e_{t-1} + \beta_2 e_{t-2} + \beta_{t-m} e_{t-m} \tag{5}$$

where the order *m* is less than 4 and is determined by AIC. From the left hand side the following characteristic equation of the system is obtained.

$$G(z) = z^4 + \alpha_1 z^3 + \alpha_2 z^2 + \alpha_3 z + \alpha_4 = \prod_{i=1}^{2} (z - z_i)(z - z_i^*)$$

Jury's stability parameter for this system is

$$F_3^- = \det\left(X_3 - Y_3\right)$$

where

$$X_3 = \begin{pmatrix} 1 & \alpha_1 & \alpha_2 \\ 0 & 1 & \alpha_1 \\ 0 & 0 & 1 \end{pmatrix}, \quad Y_3 = \begin{pmatrix} \alpha_2 & \alpha_3 & \alpha_4 \\ \alpha_3 & \alpha_4 & 0 \\ \alpha_4 & 0 & 0 \end{pmatrix}$$

and $\alpha_1 \sim \alpha_4$ are the coefficients of Eq.5.

Instead of $F_3^-$, however, we construct the following parameter combining the stability parameters.

$$F_z = \frac{F_3^-}{(F_1^-)^2} = \frac{\det\left(X_3 - Y_3\right)}{\left(1 - \alpha_4\right)^2} \tag{6}$$

The denominator is always positive at and below the flutter speed, and the numerator is Jury's stability parameter, so that $F_z$ is positive in the subcritical range and becomes zero at flutter boundary.

The analysis using a two-dimensional wing model shows that Eqs.2 and 6 have approximately the relation

$$F_z \approx T^4 F = T^4 \left[ C_2 \left( C_{L_\alpha} q \right)^2 + C_1 \left( C_{L_\alpha} q \right) + C_0 \right]$$

where $T$ is a sampling interval. Therefore the parameter $F_z$ has a similar property to the flutter margin, that is, the value of $F_z$ decreases monotonically and almost linearly toward zero in the subcritical range with the increase of the dynamic pressure.

## 3. EXTENSION OF FLUTTER PREDICTION METHOD

Though the FMDS has a superior property for the flutter prediction, it is applicable only to the two-mode system as shown in the definition. In this section, we attempt to extend it to the three-mode system.

The data having three modes is identified by the following ARMA(6, $m$) model instead of Eq.5.

$$y_t + \alpha_1 y_{t-1} + \alpha_2 y_{t-2} + \cdots + \alpha_6 y_{t-6} = e_t + \beta_1 e_{t-1} + \cdots + \beta_{t-m} e_{t-m} \tag{7}$$

Therefore, we obtain the characteristic equation

$$G(z) = z^6 + \alpha_1 z^5 + \cdots + \alpha_5 z + \alpha_6 = \prod_{i=1}^{3} (z - z_i)(z - z_i^*)$$

Here we propose a new flutter prediction parameter using Jury's stability criteria

$$F_z^{(3)} = \frac{F_5^-}{\left(F_1^-\right)^3} = \frac{\det\left(X_5 - Y_5\right)}{\left(1-\alpha_6\right)^3} \tag{8}$$

where $X_5$ and $Y_5$ are matrices whose elements consists of the coefficients of Eq.7.

$$X_5 = \begin{pmatrix} 1 & \alpha_1 & \alpha_2 & \alpha_3 & \alpha_4 \\ 0 & 1 & \alpha_1 & \alpha_2 & \alpha_3 \\ 0 & 0 & 1 & \alpha_1 & \alpha_2 \\ 0 & 0 & 0 & 1 & \alpha_1 \\ 0 & 0 & 0 & 0 & 1 \end{pmatrix}, \quad Y_5 = \begin{pmatrix} \alpha_2 & \alpha_3 & \alpha_4 & \alpha_5 & \alpha_6 \\ \alpha_3 & \alpha_4 & \alpha_5 & \alpha_6 & 0 \\ \alpha_4 & \alpha_5 & \alpha_6 & 0 & 0 \\ \alpha_5 & \alpha_6 & 0 & 0 & 0 \\ \alpha_6 & 0 & 0 & 0 & 0 \end{pmatrix}$$

We can express the denominator of Eq.8 using the characteristic roots $z_i$ as

$$1 - \alpha_6 = 1 - |z_1|^2 |z_2|^2 |z_3|^2$$

If the system is stable, the absolute value of the root is less than 1, so that the above equation has a positive value at and below the critical speed. The numerator of Eq.8 is expressed as

$$\begin{aligned} \det\left(X_5 - Y_5\right) &= \prod_{1 \le i < j \le 6} (1 - z_i z_j) \\ &= \left(1 - z_1^2\right)\left(1 - z_2^2\right)\left(1 - z_3^2\right) \\ &\quad \times |1 - z_1 z_2|^2 |1 - z_1 z_3|^2 |1 - z_2 z_3|^2 |1 - z_1 z_2^*|^2 |1 - z_1 z_3^*|^2 |1 - z_2 z_3^*|^2 \end{aligned}$$

where $z_4 = z_1^*$, $z_5 = z_2^*$ and $z_6 = z_3^*$. Therefore, it has a positive value as long as all roots locate in a unit circle, and becomes zero when one of the roots reaches a unit circle. In the flutter prediction, this means that the parameter $F_z^{(3)}$ is positive in the subcritical range and becomes zero at the speed of flutter onset.

## 4. ANALYSIS AND SIMULATION USING TWO-DIMENSIONAL WING MODEL

To study the property of $F_z^{(3)}$, we carry out the analysis using a three-degree-of-freedom wing model illustrated in Fig. 3. The values used in this model are $a$ = -0.4, $c$ = 0.6, $\mu = m/(\pi\rho b^2) = 40$, $S_\alpha/(mb) = 0.2$, $S_\beta/(mb) = 0.0125$, $r_\alpha^2 = I_\alpha/(mb^2) = 0.25$, $r_\beta^2 = I_\beta/(mb^2) = 0.00625$, $\omega_h = \sqrt{K_h/m} = 50$ (rad/sec), $\omega_\alpha = \sqrt{K_\alpha/I_\alpha} = 100$ (rad/sec) and $\omega_\beta = \sqrt{K_\beta/I_\beta}$. Here we compare the property of damping, Jury's stability parameter $F_5^-$ and 3 mode FMDS $F_z^{(3)}$. For this purpose, we use two different values for $\omega_\beta$, that is, (model 1) $\omega_\beta$=200 (rad/sec), and (model 2) $\omega_\beta$=170 (rad/sec). These models cause the different type of flutter.

The results of damping, Jury's stability parameter, and FMDS for 3-mode system $F_z^{(3)}$ are depicted in Figs. 4-6, respectively. In these figures the horizontal axis gives normalized dynamic pressure $q/q_F$, that is, the flutter boundary is $q/q_F$=1. As shown in Fig. 4, for model 1 the first and second mode are coupling and the first mode damping become unstable, whereas the third mode damping causes flutter for model 2. Model 1 is a moderate type of flutter, and model 2 is a mild type. These figures show that the critical mode can change, and the type of flutter also can change with a slight deference of the wing configuration. The critical mode damping of model 1 starts to decrease around $q/q_F$= 0.8, so that the available range for the flutter prediction is higher than $q/q_F$= 0.8.

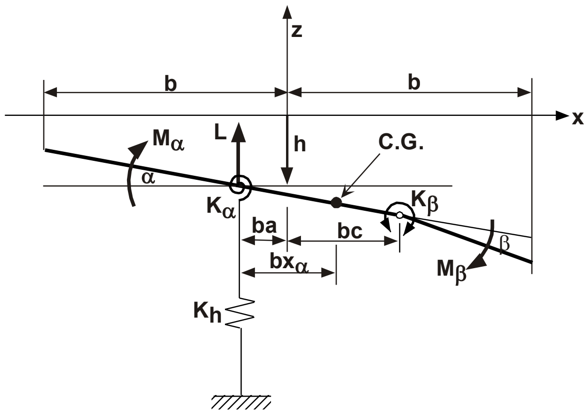


Figure 3: Two-dimensional wing model

The curve of Jury's stability parameter $F_5^-$ for both models have a similar pattern as shown in Fig. 5 and the value starts to decrease around $q/q_F$= 0.5. Figure 6 shows that also the values of the parameter $F_z^{(3)}$ has a similar pattern for both models, but unlike damping and Jury's stability parameter, $F_z^{(3)}$ decreases monotonically in the whole subcritical range. From this analysis, we can use all data in the subcritical range to predict flutter boundary by $F_z^{(3)}$. These results demonstrate that if we use $F_z^{(3)}$ as the flutter prediction parameter, we can make an accurate and reliable prediction of flutter in comparison with the method using modal damping or Jury's stability parameter.

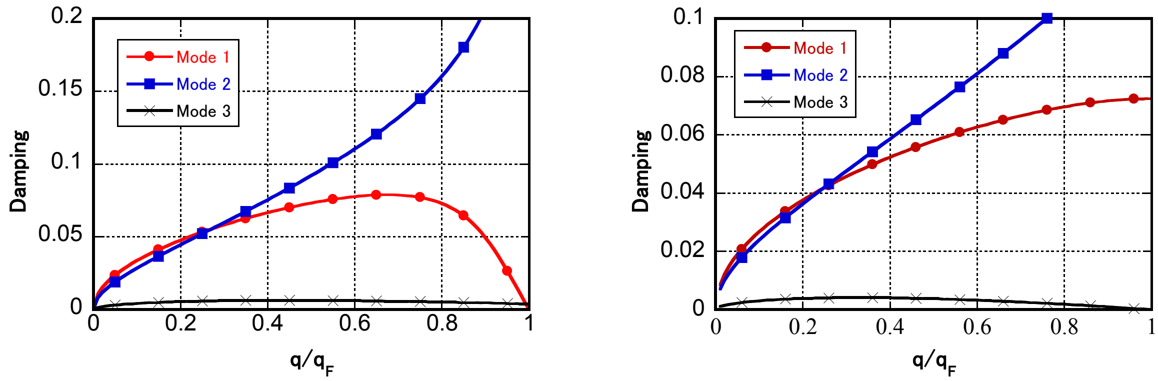


a) Wing Model 1 b) Wing Model 2

Figure 4: Damping of the wing model

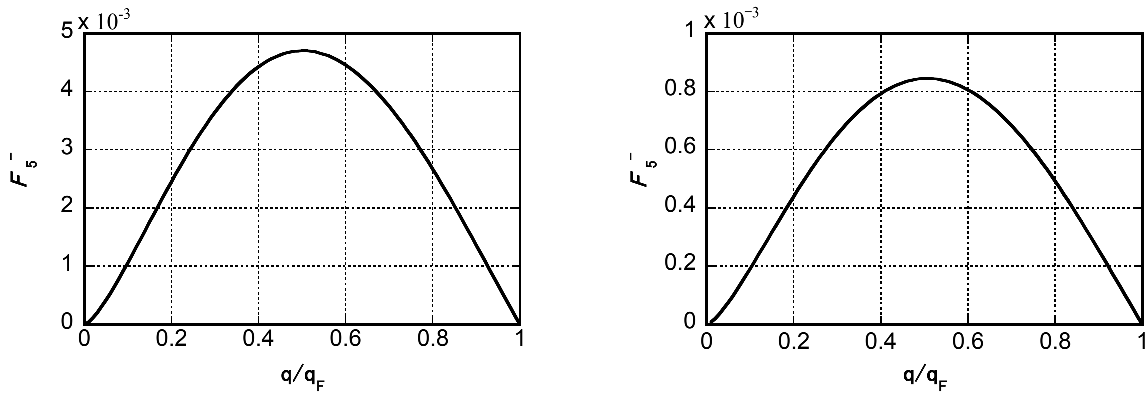


a) Wing Model 1 b) Wing Model 2

Figure 5: Jury's stability parameter $F_5^-$ of the wing model

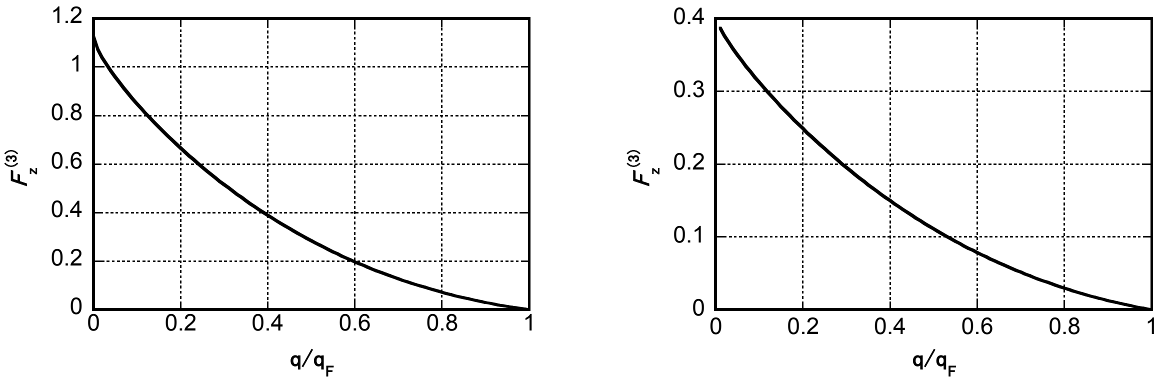


a) Wing Model 1 b) Wing Model 2

Figure 6: Parameter $F_z^{(3)}$ of the wing model

As the next analysis we use the wing model given in Ref.8, which is used for a quaternary flutter analysis of the wing of a large transport aircraft. It has four vibration mode, 1) fundamental wing bending, 2) first overtone wing bending, 3) fundamental wing torsion, and 4) aileron deflexion. Figures 7 and 8 show modal frequencies and damping, respectively. The second mode is critical and starts to decrease around $q/q_F$=0.5 as shown in Fig. 8. Here we chose 3 modes to calculate $F_z^{(3)}$, in which the second mode should be included. Figure 9 depicts the value of $F_z^{(3)}$ obtained from the lowest 3 modes, and Fig. 10 is the result obtained from 2nd to 4th mode. The value decreases monotonically toward zero for both cases. Therefore, it is obvious that $F_z^{(3)}$ is superior to damping for the flutter prediction.

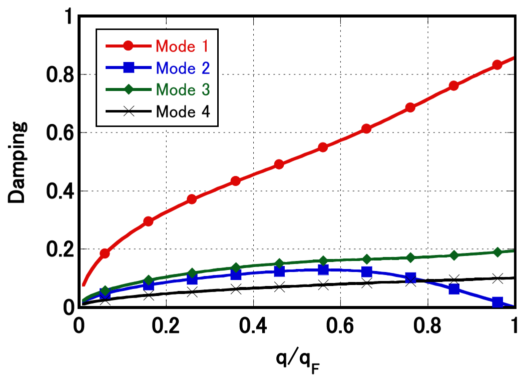


Figure 7: Modal frequencies

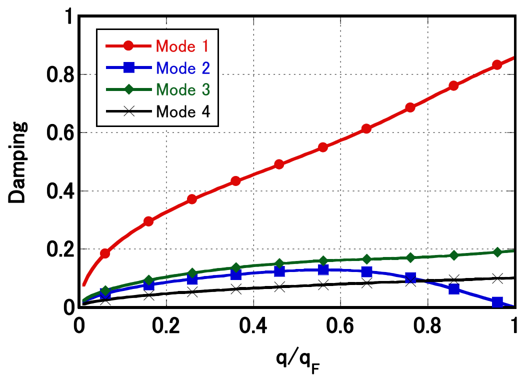


Figure 8: Modal damping

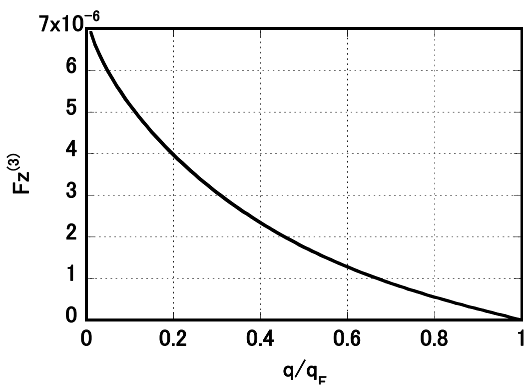


Figure 9: $F_z^{(3)}$ obtained from 1-3 modes

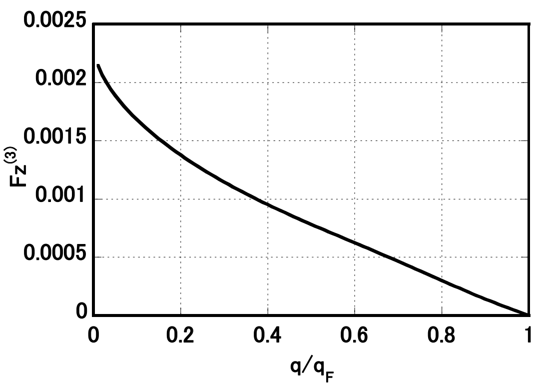


Figure 10: $F_z^{(3)}$ obtained from 2-4 modes

## 5. APPLICATION TO FLUTTER TEST DATA

To check the feasibility of this method in an actual situation, we apply it to the wind tunnel flutter test data. Figure 11 is the planform of a wing model, which is made of aluminum alloy flat plate of 2 mm thickness, and has a double-wedge at the leading and trailing edges. The response to flow turbulence is measured by strain gauge stuck on the surface of the wing.

The lowest three natural frequencies measured by the vibration test and the FEM analysis are given in Table 1. The power spectral density at $q$ = 75.7 kPa depicted in Fig. 12 shows that the data have strong noise in the lower frequency than 25 Hz. Figure 13 is the modal frequencies of the lowest 4 modes at each dynamic pressure. To include the lowest three modal frequencies and cut the low frequency noise, we apply the digital highpass filter with a cut off frequency 30 Hz.

The Mach number is fix at $M$ = 2.51 for all tests. The data are sampled at an interval $T$ = 2 ms from the analog data recorder. The flutter boundary observed by the experiment is $q_F$= 113.5 kPa, where flutter occurs by a coupling of the first and the second modes, and the second mode becomes unstable.

Wind tunnel tests are conducted (1) under the stationary condition and (2) the non-stationary condition. In the stationary tests, the data are measured at 11 points of dynamic pressure from $q$ = 75.7 to 99.4 kPa and the number of data used is $N$ = 6000, which corresponds to the measurement of 12 sec. In the non-stationary test, the dynamic pressure is swept from $q$ = 76.0 to 116.6 kPa at a rate of 2.6 kPa/sec.

Table 1 Modal frequency of wing model (Hz)

| Mode No. | FEM | Vibration test |
|---|---|---|
| 1 | 27.9 | 27.2 |
| 2 | 145.7 | 142.0 |
| 3 | 207.1 | 192.3 |

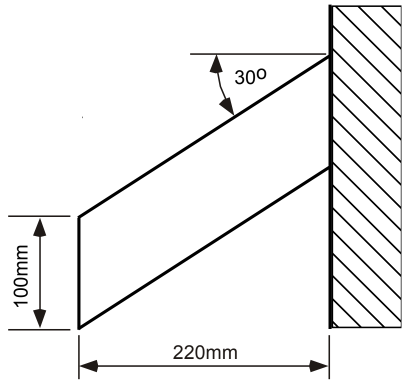


Figure 11: Planform of wing model

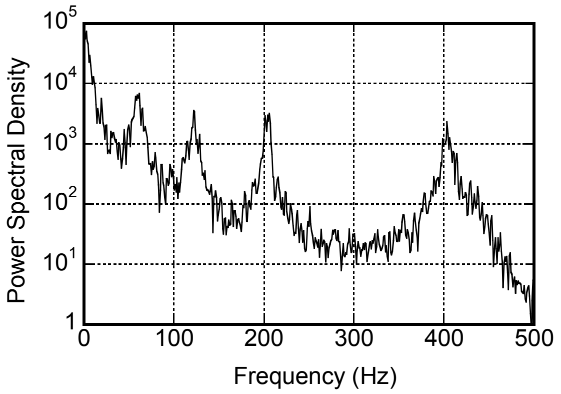


Figure 12: Power spectral density of data at $q$=75.5

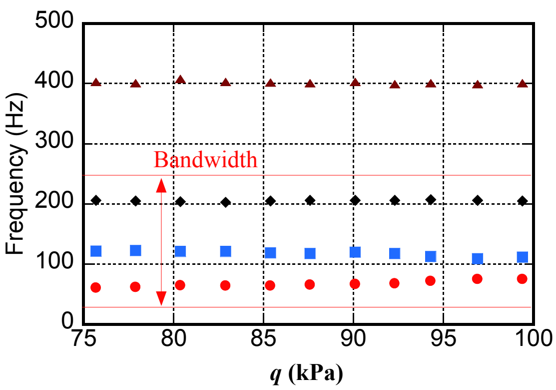


Figure 13: Modal frequencies

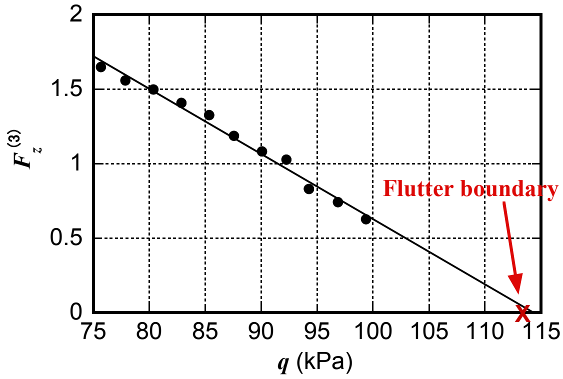


Figure 14: Estimated $F_z^{(3)}$ and the flutter prediction

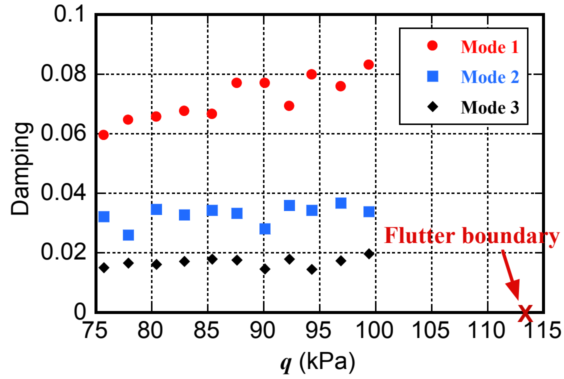


Figure 15: Estimated modal damping

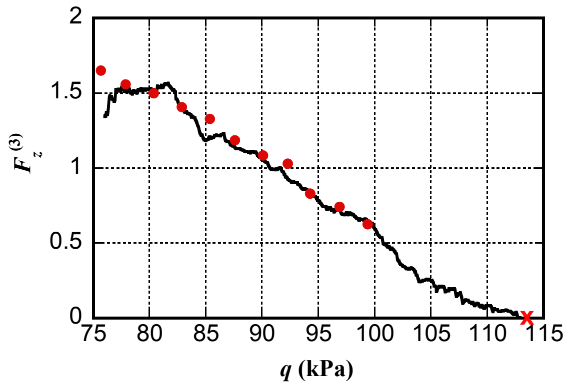


Figure 16: Estimated $F_z^{(3)}$

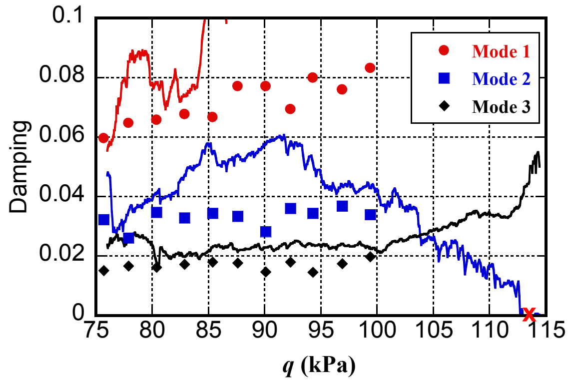


Figure 17: Estimated modal damping

### (1) Results of stationary tests

Figure 14 depicts the estimated value of $F_z^{(3)}$ plotted against the dynamic pressure. These values decrease almost linearly as the dynamic pressure increases. Therefore a linear fitting drawn by a solid straight line gives a good prediction of flutter boundary $q_F$. The actual flutter boundary observed in the experiment is marked by a symbol 'x'. The regression analysis for these estimated data gives the straight line shown in Fig.14. The intersection of this line with the horizontal axis gives the prediction of the flutter boundary, that is, $\hat{q}_F = 114.3$ kPa, which is 0.7% higher than the actual value. The goodness of fit for this regression line is $R^2$=0.986. This means that the linear fitting is reasonable.

In Fig.15 the estimated values of modal damping are depicted. The first mode has a little upward trend, and the other two modes show no trend in evidence from the tests in this range. Therefore, it is impossible to predict the flutter boundary, the point shown by 'x', based on these estimated values. We need to conduct the tests at higher dynamic pressure than this to predict the flutter boundary based on the modal damping.

### (2) Results of non-stationary test

For non-stationary data, we use a recursive identification procedure to estimate the parameters in real time, in which the coefficients of the ARMA model are updated at every sampling instance, and the value of $F_z^{(3)}$ and the modal damping is also renewed. The estimation result of $F_z^{(3)}$ is given in Fig.16, where circle symbols are the values estimated in the stationary tests. This figure shows that the values estimated recursively on a real-time procedure are the similar as the one of the stationary case, and decreases almost linearly toward zero. From this result, $F_z^{(3)}$ is an effective parameter to monitor the stability margin using with the a real-time estimation method, and gives a accurate and reliable prediction of flutter based on the recursively estimated values.

The real-time estimation of modal damping, however, gives quite different values from the results of the stationary tests as shown in Fig.17, which shows that the estimation of damping is sensitive to noise or test condition. Though the accuracy of values estimated is not clear, the second mode damping starts to decline around $q$=90 kPa. But we are not sure that these estimations are reliable or not.

## 6. CONCLUDING REMARKS

A new flutter prediction parameter applicable to the three-mode system was proposed. The analysis using wing models with three- and four-degrees of freedom showed that the value decreased monotonically and became zero at the flutter speed. Depend on a wing configuration, the critical mode changes, while $F_z^{(3)}$ was not affected. Furthermore, the feasibility for actual flutter tests was examined by the analysis of the wind tunnel test data under the stationary and non-stationary conditions, whereas damping method did not work for the same test data.

For the two-mode FMDS, we have derived approximately the relation between $F_z$ and the dynamic pressure $q$ through Zimmerman's Flutter Margin. However, we have no such relation for the parameter $F_z^{(3)}$ in this moment, and that is a problem we have to solve from now on. Also we need to consider how to expand FMDS to the system higher than 3-mode based on the framework of Jury's stability criterion.

## REFERENCES


1) Zimmerman, N. and Weissenburger, J. : Prediction of Flutter Onset Speed Based on Flight Testing at Subcritical Speeds, *J. Aircraft*, Vol. 1, No. 4, pp 190-202, 1964.

2) Price, S. and Lee, B. : Evaluation and Extension of the Flutter Margin Method for Flight Flutter Prediction, *J. Aircraft*, Vol.30, No.3, pp.395-402, 1993.

3) Matsuzaki, Y. and Ando, Y. : Estimation of Flutter Boundary from Random Responses due to Turbulence at Subcritical Speeds, *J. Aircraft*, Vol.18, No.10, pp.862-868, 1981.

4) Torii, H. and Matsuzaki, Y. : Flutter Margin Evaluation for Discrete-Time Systems, *J. Aircraft*, Vol. 38, No. 1, pp 42-47, 2001.

5) Bae, J. et al. : Extension of Flutter Prediction Parameter for Multimode Flutter Systems, *J. Aircraft*, Vol.42, No.1, pp.285-288, 2005.

6) McNamara, J. and Friedmann, P. : Flutter-Boundary Identification for Time-Domain Computational Aeroelasticity, *AIAA Journal*, Vol.45, No.7, pp.1546-1555, 2007.

7) Jury, I. E. Pavlidis, T. :Stability and aperiodicity constraints for system design, *Trans. Circuit Theory*, Vol.10, pp.137-141, 1963.

8) Collar, A. R. and Simpson, A. :Matrices and Engineering Dynamics, Ellis Horwood Ltd., London, 1987.